Critical Temperature Sensor Based on Spiking Neuron Models

Gessyca Maria Tovar, Tetsuya Hirose, Tetsuya Asai, and Yoshihito Amemiya

Graduate School of Information Science & Technology, Hokkaido University

Kita 14, Nishi 9, Kita-ku, Sapporo, 060-0814, Japan
Email: gessyca@sapiens-ei.eng.hokudai.ac.jp, hirose@sapiens-ei.eng.hokudai.ac.jp,
asai@sapiens-ei.eng.hokudai.ac.jp, amemiya@sapiens-ei.eng.hokudai.ac.jp

Abstract
We developed a subthreshold CMOS circuit whose dynamical behavior, e.g., oscillatory or stationary behaviors, changes at a given threshold temperature with the aim of the development of low-power and compact temperature switch devices on monolithic ICs. The threshold temperature is set to a desired value by adjusting an external bias voltage. The circuit consists of two pMOS differential pairs, capacitors, a current reference circuit with low-temperature dependence, and two off-chip resistors.

1. Introduction

Temperature control is fundamental in various electronic systems. There are several passive and active sensors for measuring system temperature, including thermocouples, resistive temperature sensors, thermistors, and silicon temperature sensors [1]. Among present temperature sensors, a thermistor that has positive temperature coefficients (PTC) is widely used because it exhibits a sharp increase of its resistance at a specific temperature. It is suitable for implementation in temperature control systems that make decisions, such as over-temperature shutdown, turn-on/off cooling fan, temperature compensation, or general-purpose temperature monitor.

Temperature characteristics of PTC thermistors made from ceramics, such as sintered metal oxides, are based on its material characteristics and its relative proportions [1], [2]. Electrical resistivities of PTCs are shifted by a phenomenon called leaching, which occurs during the soldering process. In addition to the resistance shift, leaching causes degradation of the solder-electrode and electrode-semiconductor bond, which may result in thermistors having greatly reduced stability and reliability. Therefore, it is difficult to build a PTC thermistor on monolithic ICs, which prevents us from developing on-chip temperature control systems.

We developed an analog circuit that has a sharp transition characteristic similar to that of PTC thermistors. Key features of the circuit include low-power subthreshold operation of MOSFETs, extended range of threshold temperature, and small packages.

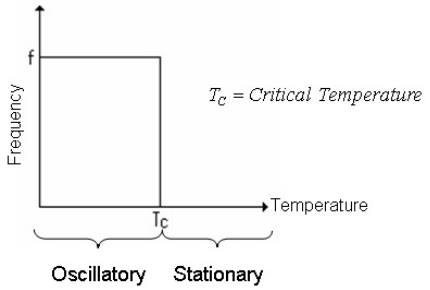

Fig. 1: Critical temperature sensor operation model

2. The Model

Temperature increase causes a regular and reproducible increase in the frequency of pacemaker potential in most *Aplysia* and *Helix* excitable neurons [3]. The Br-type neuron, located in the right parietal ganglion of *Helix pomatia*, only shows its characteristic bursting activity between 12 and $30\,^{\circ}C$. Outside this range, the burst pattern disappears and the action potentials become regular. In other words, excitable neurons can be used as a sensor to determine the temperature range in a natural environment.

There are many excitable neuron models, but only a few of them were previously implemented on CMOS LSIs, e.g., silicon neurons that emulate cortical pyramidal neurons [4], FitzHugh-Nagumo neurons with negative resistive circuits [5], artificial neuron circuits based on by-products of conventional digital circuits [6]-[8], and ultralow-power subthreshold neuron circuits [9]. We developed a model based on the Wilson-Cowan system [10] because of ease of theoretical analysis and subthreshold CMOS implementation.

Figure 1 shows the temperature sensor operation model. The temperature sensor consists of a nonlinear oscillator that changes its state e.g.., oscillatory or stationary states when it receives an external perturbation (temperature).

The dynamics of the temperature sensor can be expressed as:

$$\tau \dot{u} = -u + \frac{e^{u/A}}{e^{u/A} + e^{v/A}} \qquad (1)$$

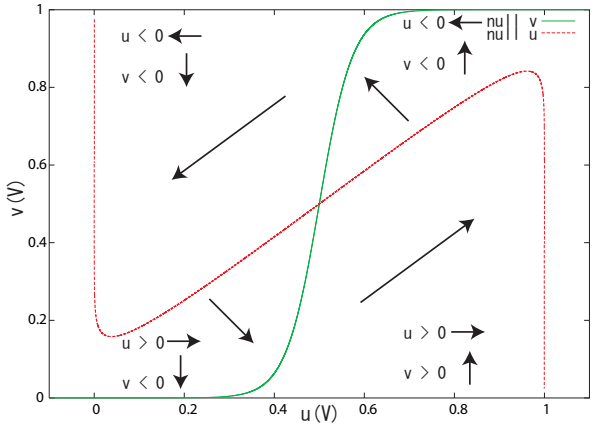

Fig. 2: *u* and *v* nullclines with vector field direction

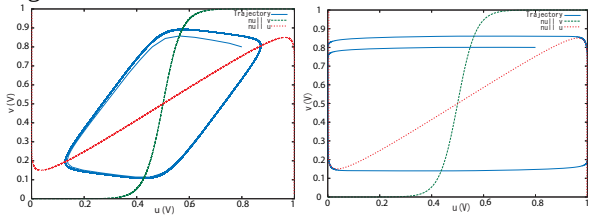

a b

Fig. 3: Trajectory when a) τ =1 and b) τ <<1

and

$$\dot{v} = -v + \frac{e^{u/A}}{e^{u/A} + e^{\theta/A}} \qquad (2)$$

where τ is the time constant, A is a constant proportional to temperature and θ is a variable. The second term of the r.h.s. of Eq. (1) is the sigmoid function, a mathematical function that produces an S-shaped (sigmoid) curve.

To analyze the system operation, we must calculate the nullclines, which are curves in the phase space where $\dot{u}$ and $\dot{v}$ are zero. Nullclines divide the phase space into four regions, and in each region, the vector field follows a specific direction. On the u nullcline, the direction of the vector is vertical, while on the v nullcline, it is horizontal. Figure 2 shows u and v nullclines and the vector field in each region.

The trajectory also depends on τ, which modifies the velocity field of u. In eq. (1), if τ is large, the value of u decreases, and for small τ, u increases. Figures 3-a and b show trajectories when τ =1 and τ <<1. The trajectory of u is much faster than that of v, so only close to the u nullcline direction of movement other then horizontal is possible.

To explain the operation of the system, let us suppose that θ is set at certain value, where the critical temperature (T_c) is $27°C$. The critical temperature represents the threshold temperature we want to measure.

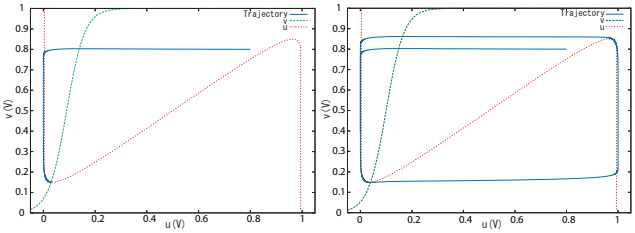

a b

Fig. 4: *u* and *v* nullclines when a) system is stable and b) system is oscillatory

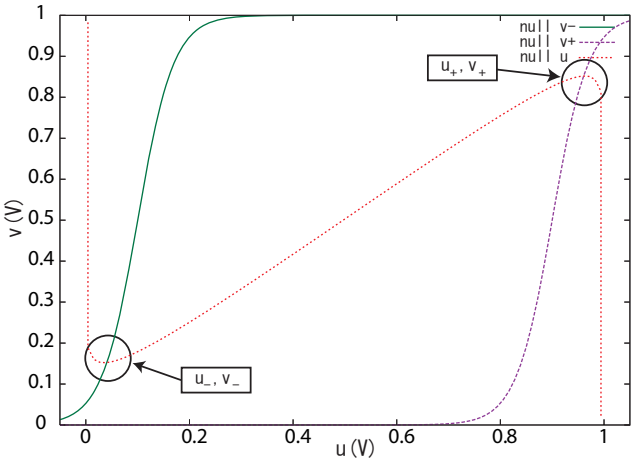

Fig. 5: *u* and *v* local minimum and maximum

When θ changes, the v nullcline changes its position in the phase space to a point where the system will be stable as long as the temperature is higher than T_c because the system is unstable only when fixed point exists in a negative resistive region of the u nullcline. The fixed point represents the intersection point of the u and v nullclines. At this point, the trajectory stops because the vector field is zero. On the other hand, when the temperature is below T_c, the nullcline and the fixed point change. The trajectory does not pass through the point, and the system starts oscillating. Figures 4-a and b show the trajectories when the system is stable and oscillatory.

The local minimum (u_-, v_-) and local maximum (u_+, v_+) where the nullclines intersect are given by:

$$u_\pm = \frac{1 \pm \sqrt{1-4A}}{2} \qquad (3)$$

and

$$v_\pm = u_\pm + A\ln\left(\frac{1}{u_\pm} - 1\right) \qquad (4)$$

Figure 5 shows the local minimum and maximum represented in the phase space.

Combining the local minimum and maximum with Eq. (2), we determine a relationship between θ and temperature, given by:

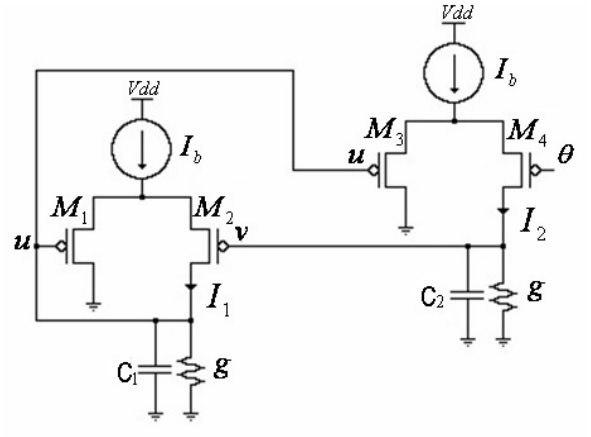

Fig. 6: Critical temperature sensor circuit

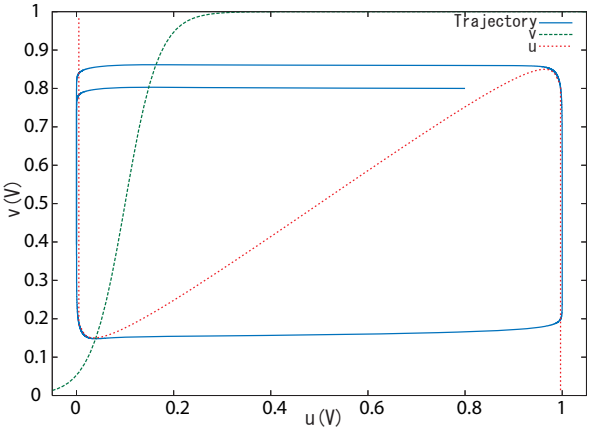

Fig. 7: Numerical simulation of nullclines and trajectory

$$\theta_{\pm} = u_{\pm} + A\ln\left(\frac{1}{v_{\pm}} - 1\right). \tag{5}$$

3. The circuit

Figure 6 shows our critical temperature sensor circuit, which consists of two pMOS differential pairs (M_1-M_2 and M_3-M_4), two capacitors (C_1 and C_2), a current reference circuit (I_b) [11], and two off-chip metal-film resistors (g) with low-temperature dependence.

Differential pairs subthreshold currents I_1 and I_2 are given by:

$$I_1 = I_b \frac{e^{\kappa u / v_T}}{e^{\kappa u / v_T} + e^{\kappa v / v_T}} \tag{6}$$

and

$$I_2 = I_b \frac{e^{\kappa u / v_T}}{e^{\kappa u / v_T} + e^{\kappa \theta / v_T}}, \tag{7}$$

therefore, circuit dynamics can be determined by applying Kirchhoff's Current Law to both differential pairs, which is represented as follows:

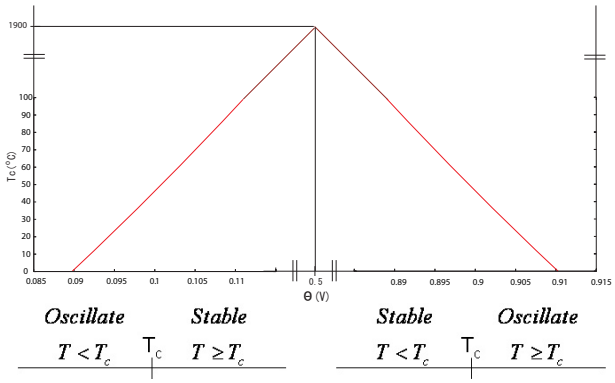

Fig. 8: Relation between $\theta_{\pm}$ and T_c

$$c_1\dot{u} = -gu + \frac{I_b e^{\kappa u / v_T}}{e^{\kappa u / v_T} + e^{\kappa v / v_T}} \tag{8}$$

and

$$c_2\dot{v} = -gv + \frac{I_b e^{\kappa u / v_T}}{e^{\kappa u / v_T} + e^{\kappa \theta / v_T}}, \tag{9}$$

where κ is subthreshold slope, v_T is thermal voltage (v_T = KT/q), K is Boltzmann's constant, T is temperature, q is elementary charge, c_1 and c_2 are the capacitance, they represent the time constants, and θ is bias voltage. The circuit changes its dynamical behavior between stable and oscillatory at a given critical temperature, which is set by adjusting the bias voltage θ.

Numerical simulations were conducted by setting c_1 and c_2 at 0.1 and 10 pF, respectively, g at 1 nS, and reference current I_b at 1 nA. Figure 7 shows the nullclines and trajectory of the circuit with θ set at 0.5 V and T at $27°C$; the system is in an oscillatory state.

Setting T_c and changing θ until the system changes its state, we established a numerical relation between T_c and θ: θ_- for u and v local minimums and θ_+ for u and v local maximums. Figure 8 shows the relation between $\theta_{\pm}$ and T_c. When θ_- is used to set T_c, the system is stable at temperatures higher than T_c; while when θ_+ is used, the system is stable when the temperature is lower than T_c and oscillatory when it is higher than T_c.

Figure 9 shows the numerical nullclines and trajectory using θ_-, T is higher than T_c; and Fig. 10 shows the numerical nullclines and trajectory using θ_+, T is lower than T_c.

We used SPICE simulation to determine circuit operation. We simulated circuit nullclines and changed

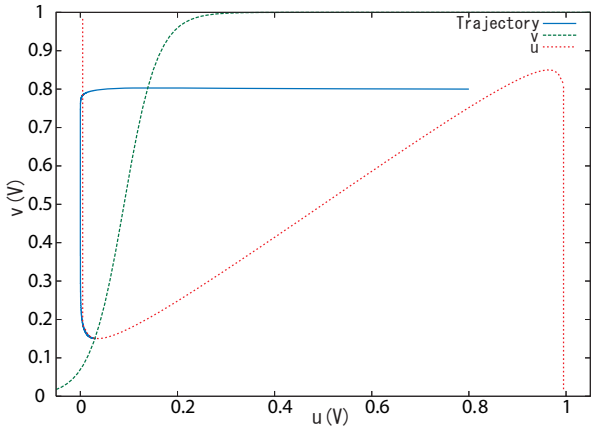

Fig. 9: Numerical nullclines and trajectory by setting T_c using θ_-

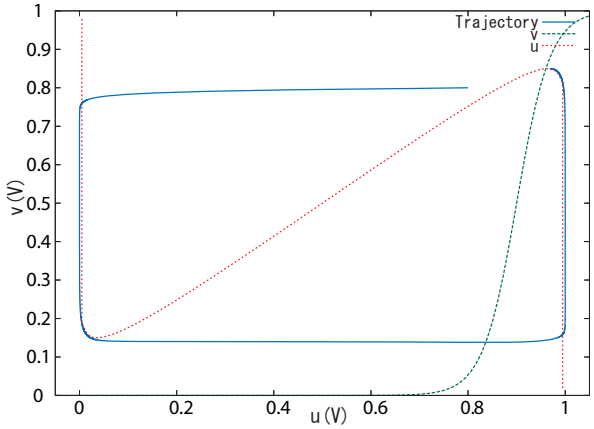

Fig. 10: Numerical nullclines and trajectory by setting T_c using θ_+

θ to determine circuit operation in stable and oscillatory states. For the θ vs. T_c relationship, we found a mismatch between the numerical and circuit simulations. This difference might be due to all parameters that we included in the SPICE simulation but omitted in the numerical and theoretical equations. Many of these parameters might have temperature dependence; therefore, their value changes with temperature, and as a result of this change, the T_c characteristic changes.

4. Summary

We developed a subthreshold CMOS circuit whose dynamical behavior, e.g., oscillatory or stationary behaviors, changes at a given threshold temperature. Threshold temperature was set to a desired value by adjusting bias voltage. The circuit's operation was investigated through theoretical analysis and extensive numerical simulations.

5. References

[1] W. Gopel, J. Hesse, and J. N. Zermel, *Sensors. A comprehensive survey*, Vol. 4, VCH, *Thermal sensors* (T. Ricolfi and J. Scholz, Eds.), 1990, pp. 235–239.

[2] C. C. Wang, S. A. Akbar, and M. J. Madou, "Ceramic based resistive sensors," J. Electroceramics, Vol. 2, No. 4, pp. 273–282, 1998.

[3] D. S. Fletcher and L. J. Ram, "High temperature induces reversible silence in Aplysia R15 bursting pacemaker neuron," Comp. Biochem. Physiol., Vol. 98A, pp. 399–405, 1990.

[4] R. Douglas, M. Mahowald, and C. Mead, Neuromorphic analogue VLSI, *Ann. Rev. Neurosci*., 18, 1995, 255–281.

[5] B. L. Barranco, E. S. Sinencio, A. R. Vazquez, and J. L. Huertas, A CMOS implementation of FitzHugh-Nagumo neuron model, *IEEE J. Solid-State Circuits*, 26, 1991, 956–965.

[6] S. Ryckebusch, J. M. Bower, and C. Mead, Modelling small oscillating biological networks in analog VLSI, in *Advances in Neural Information Processing Systems 1*, (D. S. Touretzky, Ed., Los Altos, CA: Morgan Kaufmann, 1989, 384–393).

[7] A. F. Murray, A. Hamilton, and L. Tarassenko, Programmable analog pulse-firing neural networks, in *Advances in Neural Information Processing Systems 1*, (D. S. Touretzky, Ed., Los Altos, CA: Morgan Kaufmann, 1989, 671–677).

[8] J. L. Meador and C. S. Cole, A low-power CMOS circuit which emulates temporal electrical properties of neurons, in *Advances in Neural Information Processing Systems 1*, (D. S. Touretzky, Ed., Los Altos, CA: Morgan Kaufmann, 1989, 678–685).

[9] T. Asai, Y. Kanazawa, and Y. Amemiya, A subthreshold MOS neuron circuit based on the Volterra system, *IEEE Trans. Neural Networks*, 14(5), 2003, 1308–1312.

[10] H. R. Wilson and J. D. Cowan, Excitatory and inhibitory interactions in localized populations of model neurons, *Biophys. J*., Vol. 12, pp. 1–24, 1972.

[11] T. Hirose, T. Matsuoka, K. Taniguchi, T. Asai, and Y. Amemiya, "Ultralow-power current reference circuit with low-temperature dependence," IEICE Transactions on Electronics, Vol. E88-C, No. 6, pp. 1142–1147 (2005).